The Stark Model: An Exact, Closed-Form Approach to Low-Thrust Trajectory Optimization

Gregory Lantoine* and Ryan P. Russell†
Georgia Institute of Technology, Atlanta, Georgia, 30318, USA

August 18, 2009

Abstract

Low-thrust propulsion is becoming more popular for space missions because of its efficient propellant usage. However the optimization of the resulting trajectories remains a very challenging task, especially to obtain precise optimal solutions. In this paper, we study the Stark model, an exact, closed-form formulation to parameterize the low-thrust problem by subdividing the trajectory into two-body segments subjected to Newtonian gravitation plus an additional uniform force of constant magnitude and direction. Compared to existing analytic methods, this model can take into account more accurately the effect of thrusting and the full dynamics of the problem, at the expense of a slight speed overload. First, all the general types of solutions, expressed in terms of elliptic integrals, are described in details. Then a state-of-the-art optimization solver specially tailored to exploit the structure of the problem is used to take advantage of those closed-form solutions. Preliminary numerical results are presented and compared to existing algorithms to illustrate the performance and the accuracy of our approach. It is believed that our method can, in most cases, eliminate the necessity to numerically propagate equations of motion even in perturbed environments.

1 Introduction

Low-thrust propulsion presents great benefits and is increasingly being considered for space missions. It can significantly enhance mission feasibility by using propellant more efficiently, and greatly improve mission feasibility by providing more control capability. To explore the trade space in a timely and efficient manner, the conceptual design of a low-thrust mission requires fast and accurate methods. In particular, one has to choose the components of the thrust force as a function of time to meet desired final conditions with minimum fuel consumption. A common robust and flexible approach is to use nonlinear programming techniques and discretize the thrust profile to directly minimize propellant mass,[1] but this can lead to a large number of control variables as low-thrust propulsion can operate for a significant part of the mission lifetime. Generally, numerical integration of a set of differential equations describing the system dynamics and the corresponding derivatives has to be performed, and the number of equations to integrate increases significantly as the number of variables increases (the so-called 'curse of dimensionality').[2] As a consequence, the search for optimized low-thrust trajectories is typically challenging and time-consuming, which prevents the designers from efficiently exploring a large number of options at the early design phase.

To overcome this issue, a widespread strategy relies on analytical closed form expressions to avoid expensive numerical integrations.[3] Petropoulos provides a complete survey of the exact analytic solutions that have been found to the planar equations of motion for a thrusting spacecraft.[4] Some of those closed-form solutions have been used in a number of preliminary studies of low-thrust mission design.[5,6] In his Ph.D. thesis,[7] Petropoulos focuses particularly on a family of analytic solutions assumed to be of a shape of an exponential sinusoid and shows that we can obtain trajectories with correct performance and near-feasible thrust profiles. In the same spirit, Bishop and Azimov obtained exact planar solutions for propellant-optimal transfer along spiral trajectories.[8] However, all those formulations are limited by unrealistic constraints on the thrust profile (for instance, the exponential sinusoid solution accounts for tangential thrust only), so they do not have general application for finding accurate optimal solutions. A more general formulation is given by Johnson who studies

*PhD Candidate, School of Aerospace Engineering, 270 Ferst Dr., AIAA Member, gregory.lantoine@gatech.edu.
†Assistant Professor, School of Aerospace Engineering, 270 Ferst Dr., AIAA Member, ryan.russell@gatech.edu.

analytic trajectories produced by a thrust vector with a constant angle with respect to the radius vector.[9] But his theory is not exact, only yielding approximate second-order solutions.

Another existing analytical technique from Sims and Flanagan models low-thrust trajectories as a series of impulsive maneuvers connected by two-body coast arcs.[10] This parameterization - referred as the Kepler model throughout this paper - can therefore take advantage of the well-known analytical expression of Keplerian motion.[11] The model is akin to using a low order Euler integration scheme on the thrust, but a highly accurate integration method on the Keplerian motion. The state-of-the-art software MALTO developed at JPL,[12] and GALLOP, developed at Purdue University,[13] are based on this approach and use non-linear programming (NLP) solvers to generate many interesting and competitive results.[14] This method can be also combined with differential dynamic programming (with the inclusion of analytic second order derivatives) for better robustness.[15] However, while n-body, oblateness, and other perturbations can be also approximated by discrete force impulses, the model is best suited for near Keplerian problems. For problems with strong or non-stationary perturbations (which is generally the case when full dynamics are considered), accuracy can be very limited unless a very fine discretization is taken. This effect can increase significantly the number of control variables, and makes the problem harder to solve and potentially reduces the interest of the approach.

Intermediate between the integrable two-body problem and the non-integrable multi-body problem sits the problem of a body moving in Newtonian field plus a constant inertial force field. We will see here that this problem is also fully integrable and analytically soluble in terms of elliptic functions. This problem has been particularly studied in physics and quantum mechanics to understand the so-called Stark effect, i.e. the shifting and splitting of spectral lines of atoms and molecules in the presence of an external static electric field. The effect is named after the German physicist Johannes Stark who discovered it in 1913.[16] Throughout this paper, we will therefore use the common expression 'Stark problem' to refer to this problem. Understanding the Stark effect is important for the analysis of atomic and molecular rotational spectra.[17,18] Exploiting this effect can also greatly enhance the utilities of some molecules.[19] In addition, the Stark problem can play the role of a model problem from which one can obtain information about the properties of atoms in interstellar space where strong electric fields are generally present.

In our context, we can take advantage of the integrability of the Stark problem by subdividing the trajectory into multiple two-body segments subjected to an additional uniform force of constant magnitude and direction. This approach can model more accurately the effect of thrusting and the full dynamics of the problem, which can be essential in the design of efficient trajectories in multi-body environments. In addition, piecewise constant thrust is a reasonable and realistic model since the thrust may not change frequently in actual implementation. Like the Kepler formulation, propagation consists solely of a sequence of Stark steps; therefore no numerical integration is necessary. Perturbations in the stark model can be approximated as constants over a segment and simply added to the thrust vector. In the same way, analytical expressions of the first- and second-order state transition matrices (STMs) can be deduced, from which we can derive the derivatives necessary for the optimization process. Combining speed and accuracy, this parameterization therefore allows the solution to a wide class of problems and limits - although does not eliminate - the pitfall of fine discretization associated with impulsive techniques.

To find in practice the optimal solution of the resulting problem, we use a powerful, recently developed, hybrid differential dynamic programming (HDDP) algorithm.[20] It combines several NLP techniques with differential dynamic programming, a proven second-order method based on Bellman's Principle of Optimality and successive minimization of quadratic approximations.[21,22] For this problem, HDDP provides several advantages over classical NLP solvers, like SNOPT.[23] When the number of unknowns is large (which is often the case in low-thrust problems due to thrust discretization), NLP methods tend to become computationally prohibitive and difficult to converge, even with sparse capabilities. On the other hand, HDDP is not as sensitive to high dimensional problems because it transforms those large problems into a succession of low dimensional problems. In addition, HDDP directly employs STMs in the optimization process, and we can therefore take advantage of the analytic expressions of the STMs of the Stark problem in a very transparent way. The same basic principle has been previously applied to integrate the Kepler formulation into the HDDP framework.[15]

In summary, the main goal of this study is to demonstrate the value of using a Stark formulation in low-thrust trajectory optimization. In addition, we aim to deepen the understanding of the characteristics of the

interesting Stark problem, one of the few exactly solvable problems in celestial mechanics. Therefore, this paper will be divided into four parts. It begins with a thorough review of previous work regarding the Stark model over the past three centuries. The second section is devoted to the derivation of the analytical expressions to the solution of the Stark problem (noting that most of the existing literature lacks explicit solutions). The derivations lead naturally to an understanding of the principal properties of the solutions. The third part is focused on a detailed comparison of speed and accuracy of the Kepler and Stark formulations to assess the utility and applicability of both methods. The last section considers the application of the Stark formulation to low-thrust trajectory optimization using HDDP. A relevant numerical example is presented consisting of a simple orbit-to-orbit transfer (with and without perturbations taken into account).

2 Historical survey

The common integrable problems of celestial mechanics are easily counted, namely, the Kepler problem and the Euler problem (two center Newtonian gravitational motion). The Stark problem is less known to the space flight community, but is indeed an integrable example. In fact, the Stark problem can be viewed as the limiting case of the Euler problem when, while keeping fixed one of the two masses, the other goes to infinity (its mass approaches infinity as well). The remarkably small number of integrable problems explains why the Stark problem has received special attention over almost two and one-half centuries, with occasionally quite intense studies. In addition, in physics, this problem is of great interest to describe the characteristics of atoms in a constant electric field, which drove more researchers to analyze this problem. We now give a brief historical survey of the Stark problem's evolution.

The Stark problem was shown to be integrable first by Lagrange who reduced it to quadratures at the end of the 18th century.[24] Although elliptic functions were not known at his time, Lagrange's analysis and reduction is very elegant, and he has already the intuition that the solution can be expressed with some transcendental functions ("rectification of conic sections"). Lagrange also points out that the Stark problem is far from being a particular case of the Euler problem and that a dedicated analysis is necessary.

In the middle of the 19th century, two mathematicians, Jacobi and Liouville, give a crucial contribution towards a more a rigorous treatment of the Stark problem. Their work represents the mathematical foundation that all later studies build upon, including this paper. Following the work of Hamilton on his General Method in Dynamics,[25] Jacobi derives a general procedure for the study of dynamical systems through the Hamilton-Jacobi equation. Jacobi also found that the Stark system admits the separation of variables in the parabolic coordinates and formulates the Hamilton-Jacobi equation for the problem in these coordinates. Complementing the ideas of Jacobi, Liouville comes up with sufficient conditions for separability of dynamical systems (at the origin of the notion of Liouville integrability), and noted that most of the known integrable problems, including the Stark problem, met his conditions for separability.[26]

At the beginning of the 20th century, the Stark problem received other attention due to the first observations of the Stark effect. Within a decade of the appearance of Bohr's quantum theory, this effect was first explored to explain some characteristics of the hydrogen atom in a state excited by a homogeneous electric field.[27–29] Most authors relied on the same parabolic coordinates and separation of variables to characterize the motion of the electron (subjected to the inverse square law Coulomb field and an homogeneous field) in a hydrogen atom, whether from a classical or quantum mechanics perspective. On one hand, Born stays in a classical mechanics context to show that previous theories of the Stark problem are particularly powerful to find transition frequencies of excited systems, but he only finds approximate solutions using Fourier series.[30] On the other hand, Froman provides a comprehensive review of all major studies of the Stark effect from a quantum mechanics point of view.[31] In connection with the development of wave mechanics, it is shown that the Schrodinger equation for a one-electron system in a homogeneous electric field is also separable in parabolic coordinates. This analogy between the treatment of the Stark problem in quantum and classical mechanics is remarkable. More recently, the Stark problem is extended by considering a charged particle moving in the field of one localized dyon inside a homogeneous electric field (refered to as the MICZ-Kepler-Stark system).[32] As in the nominal case, this also is an integrable system, which allows separation of variables in parabolic coordinates.

Another important milestone in the history of the Stark problem is the work of Kirchgraber in the seven-

ties. He is concerned (like us) with handling perturbations of the Kepler problem and contrary to previous authors who all use parabolic coordinates, he uses the so-called KS-variables to show that the Stark problem is separable and to describe it analytically.[33] However, the required change of variables is a complicated nonlinear transformation which is likely to be computationally slow and presents less physical insight than previous transformations. Later, using Kirchgraber's method, Rufer is the first to apply the Stark formulation to trajectory optimization,[34] but the cases are very limited, analytic derivatives are not considered, and no results on performance and speed are presented. Surpringly, this idea was not further explored by any authors until today.

Following the launch of Sputnik, the Russian scientific community took also interest in this problem and is at the origin of extensive studies. In fact, in a relatively short time interval, we can approximate solar pressure as a constant force both in magnitude and direction, and the Stark problem is therefore useful to understand the motion of a satellite perturbed by solar radiation. In this context, Isayev derives an analytical theory of motion for a balloon-satellite perturbed by a constant solar pressure.[35] More generally, Beletski characterizes (incompletely) the different types of orbits that can be encountered in the planar Stark problem.[36] Later, noting that all previous methods require to adjust the initial physical coordinate system to the specified constant force, another Russian author, Poleshchikov, has the idea to employ the KS-variables to regularize the equations of motion.[37]

More recently, the work of Cordani is also worth mentioning.[38] He provides a brief discussion of the Stark problem as an integrable perturbation of the Kepler problem in parabolic coordinates. He further presents an inspirational long analysis of the Euler problem. Less useful for our formulation, Vozmischeva generalizes the context of the Stark problem to a space of constant curvature.[39] Finally, in modern astrophysics, some researchers are now using an analytical Stark propagator to facilitate very long-term numerical integrations.[40]

In summary, a large number of studies have covered the Stark problem. However, a curious common feature of all those works is that no complete listing of the solutions has been presented. The problem of transforming the resulting quadratures to Legendre canonical form in order to derive the solution in terms of elliptic functions is the crux of the matter. The next section is therefore devoted to this derivation, along with a complete presentation and analysis of all the solutions of the Stark problem.

3 Analysis of the Stark Problem

In spite of the impressive progress on the power of computer-based numerical computations, qualitative methods of studying integrable dynamical systems are still today of considerable interest. Explicit closed-form formulas often lead to general laws of behavior and improved insight of a particular problem. In this section, we will build upon traditional methods of dynamics through a Hamiltonian approach to describe in details the Stark problem and derive the desired analytical expressions of the solution. At the end, the first complete listing of all solutions, for both two-dimensional and three-dimensional cases, is presented along with their specific properties.

3.1 Two-dimensional case

3.1.1 Formulation of the problem

To simplify the analysis and gain insight to the problem, the planar case is considered first. In the x-y plane, we consider the motion of an arbitrary point P in the gravitational field induced by a body at the origin, and subjected to an additional constant inertial force. Without loss of generality, we can assume that this force is in the y-direction since the arbitrary direction can be arrived by means of a trivial coordinate rotation.

The corresponding planar equations of motion are the following:

$$\begin{cases} \ddot{x} = -\frac{\mu}{r^3} x \\ \ddot{y} = -\frac{\mu}{r^3} y + \epsilon \end{cases} \tag{1}$$

where $r = \sqrt{x^2 + y^2}$ and ϵ is a parameter fixing the value of the constant force. Note that the perturbing force is not supposed to be small.

The corresponding potential function per unit mass at point P is given by $V = -\frac{\mu}{r} + \epsilon y$, and the kinetic energy per unit mass is classically $T = \frac{1}{2}(\dot{x}^2 + \dot{y}^2)$. It follows that the energy per unit mass, or Hamiltonian H, takes the form:

$$H = T + V = \frac{1}{2}(\dot{x}^2 + \dot{y}^2) - \frac{\mu}{r} - \epsilon y \tag{2}$$

According to classical dynamics theory, H is an integral of motion.

3.1.2 Reduction to quadratures

To reduce the problem to quadratures, we follow the same classical method as many authors[30, 32, 36, 38, 39, 41] who have studied the Stark problem or other integrable problems. According to Liouville, if the Hamiltonian allows separation of variables, the problem is integrable.[26] In such cases, each of the energy functions (kinetic and potential) is the sum of distinct components, where every component involves but one position coordinate. Clearly Eq. 2 shows that the Hamiltonian is not separable in Cartesian coordinates. However, previous authors have found that it becomes separable in parabolic coordinates, given by the following relations:

$$\begin{cases} \xi^2 = y + r \\ \eta^2 = -y + r \end{cases} \tag{3}$$

The name comes from the fact that the curves ξ = const and η = const are parabolas with y-axis symmetry and the origin as the focus. The choice of this coordinate system makes sense intuitively. In fact, far from the gravitational body the constant force becomes dominant over the Newtonian force and the motion in a homogeneous field executes a parabola whose axis is directed along the direction of the field.

The new potential has a singularity at $(0, 0)$, so it is better to introduce a new time variable τ by the defining relation:

$$dt = (\xi^2 + \eta^2)d\tau = 2rd\tau \tag{4}$$

Generally speaking, this regularization procedure is often required for problems of celestial mechanics to avoid divergence close to the attracting center. With prime denoting differentiation with respect to τ, the new velocities (also called generalized momenta in a Hamiltonian mechanics context) are written:

$$\begin{cases} \xi^{'} = \frac{\partial \xi}{\partial \tau} = (\xi^2 + \eta^2)\dot{\xi} \\ \eta^{'} = \frac{\partial \eta}{\partial \tau} = (\xi^2 + \eta^2)\dot{\eta} \end{cases} \tag{5}$$

The general transformation $(x, y, t) \Rightarrow (\xi, \eta, \tau)$ is sometimes called the Arnol'd duality transformation and has been used to solve other kinds of perturbed Kepler problems.[42] We could have chosen to use the KS-transformation like Kirchgraber and others,[33, 37] but as mentioned in the previous section, the formulas of inversion of the KS-transformation are complicated and likely not preferrable based on computational speed.

In terms of the new space and time coordinates, the Hamiltonian can be expressed as:

$$H = \frac{1}{2}\frac{\xi^{'2} + \eta^{'2}}{\xi^2 + \eta^2} - 2\frac{\mu}{\xi^2 + \eta^2} - \frac{1}{2}\epsilon(\xi^2 - \eta^2) \tag{6}$$

To separate the variables, we multiply Eq. 6 by $(\xi^2 + \eta^2)$ and, after manipulating the terms, we find:

$$H\xi^2 - \frac{1}{2}\xi^{'2} + \mu + \frac{1}{2}\epsilon\xi^4 = -H\eta^2 + \frac{1}{2}\eta^{'2} - \mu + \frac{1}{2}\epsilon\eta^4 \tag{7}$$

Now the left side is a function of ξ only, and the right side is a function of η only. In order for Eq. 7 to hold for all ξ and η, each of the terms must be constant. This separation constant is the second integral of motion:

$$H\xi^2 - \frac{1}{2}\xi^{'2} + \mu + \frac{1}{2}\epsilon\xi^4 = -H\eta^2 + \frac{1}{2}\eta^{'2} - \mu + \frac{1}{2}\epsilon\eta^4 = -c \tag{8}$$

Returning back to Cartesian coordinates, this constant of motion can be written:

$$c = \dot{x}(y\dot{x} - x\dot{y}) - \mu\frac{y}{r} - \frac{1}{2}\epsilon x^2 \tag{9}$$

This integral corresponds to the conservation of the generalized Laplace-Runge-Lenz vector (more commonly named eccentricity vector in celestial mechanics) in the direction of the constant external field.[43] After re-ordering again the terms, the latter equation leads to two equalities:

$$\begin{cases} \xi^{'} = +/- \sqrt{2(\frac{\epsilon}{2}\xi^4 + H\xi^2 + \mu + c)} \\ \eta^{'} = +/- \sqrt{2(-\frac{\epsilon}{2}\eta^4 + H\eta^2 + \mu - c)} \end{cases} \tag{10}$$

The sign determination will be considered later. For the moment, a positive sign is assumed and we may write:

$$\tau = \int \frac{d\xi}{\sqrt{P_\xi(\xi)}} + \text{const} \tag{11a}$$

$$\tau = \int \frac{d\eta}{\sqrt{P_\eta(\eta)}} + \text{const} \tag{11b}$$

where

$$P_\xi(\xi) = \epsilon(\xi^4 + \frac{2H}{\epsilon}\xi^2 + \frac{c+\mu}{\epsilon}) \tag{12a}$$

$$P_\eta(\eta) = -\epsilon(\eta^4 - \frac{2H}{\epsilon}\eta^2 + \frac{c-\mu}{\epsilon}) \tag{12b}$$

The problem is therefore reduced to quadratures, more specifically to elliptic integrals. The key is now to invert those integrals to find parametric expressions of the variables ξ and η in functions of fictitious time τ.

3.1.3 Integration of quadratures

To find the desired parametric expressions of the solution $\xi(\tau)$ and $\eta(\tau)$, we must perform analytically the integration of the two quadratures, and inverse the result. For that, we take inspiration of the general method described by Bowman.[44] By suitable transformation of variables, any elliptic integral of the form of $\int \frac{dX}{\sqrt{P(X)}}$ where $P(X)$ is a quartic polynomial, can be reduced to Legrendre's standard form of an elliptic integral of first kind $\int \frac{dZ}{\sqrt{1-Z^2}\sqrt{1-k^2Z^2}}$ where k is called the modulus and must verify $0 \leq k \leq 1$. This last integral is inversed and solved through the Jacobi elliptic function $Z = sn(\tau + c)$ where c is an integration constant. Although this transformation seems a simple algebraic problem, it is in practice quite a challenging exercise since the transformations reducing Eq. 11a and Eq. 11b to canonical form depend on the values taken by the roots of the quartic polynomial. We must therefore distinguish several cases. The complete procedure for reducing the P_ξ and P_η equations is presented now in details for the first time.

The P_ξ equation

Since P_ξ is a biquadratic polynomial, computing the roots is facilitated by the classical transformation $\psi_\xi = \xi^2$. P_ξ is then reduced to a simple quadratic in ψ_ξ:

$$P_\xi(\psi_\xi) = \epsilon(\psi_\xi^2 + \frac{2H}{\epsilon}\psi_\xi + \frac{c+\mu}{\epsilon}) \tag{13}$$

For a quadratic equation, the sign of the discriminant Δ_ξ determines the nature of the roots:

$$\Delta_\xi = \left(\frac{2H}{\epsilon}\right)^2 - 8\frac{c+\mu}{\epsilon} \tag{14}$$

Case A: $\Delta_\xi > 0$

A positive discriminant means that P_ξ has two real roots in ψ:

$$\begin{cases} \psi_\xi^+ = \frac{1}{2}(-\frac{2H}{\epsilon} + \sqrt{\Delta_\xi}) \\ \psi_\xi^- = \frac{1}{2}(-\frac{2H}{\epsilon} - \sqrt{\Delta_\xi}) \end{cases} \tag{15}$$

To factorize P_ξ in terms of ξ, different cases must be distinguished depending on the signs of ψ_ξ^+ and ψ_ξ^- (since ξ is the square root of ψ_ξ).

Case A.1: $\psi_\xi^+ > 0$, $\psi_\xi^- > 0$

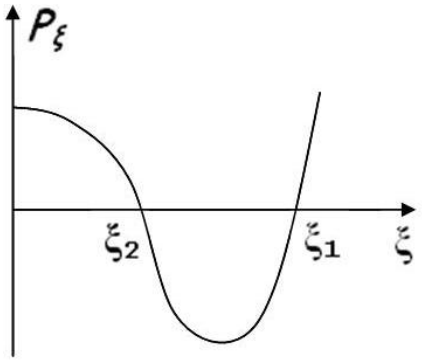

Figure 1: Representative plot of polynomial P_ξ with two real positive roots.

In that case, P_ξ has 4 real roots. The two positive roots satisfy:

$$\begin{cases} \xi_1^2 = \psi_\xi^+ \\ \xi_2^2 = \psi_\xi^- \end{cases} \tag{16}$$

where $\xi_1^2 > \xi_2^2$.

It is obvious from Eq. 11a that the motion is feasible only in the regions of a space in which the condition $P_\xi > 0$ is met. From the illustrative plot of P_ξ in figure 1 (since P_ξ is symmetric, only the positive x-axis is shown), ξ must satisfy the following two inequalities

$$\begin{cases} \xi^2 < \xi_2^2 \\ \xi^2 > \xi_1^2 \end{cases} \tag{17}$$

Those conditions must be met at all times, in particular at starting conditions. Hence we must distinguish again two sub-cases.

Case A.1.1: $\xi_0^2 < \xi_2^2$

P_ξ takes the following factorized form:

$$P_\xi(\xi) = \epsilon(\xi_1^2 - \xi^2)(\xi_2^2 - \xi^2) \tag{18}$$

The integration is facilitated by the introduction of an auxiliary dependent variable α, defined by $\xi = \xi_2\alpha$, which yields the integral:

$$\tau = \int \frac{d\alpha}{\sqrt{\epsilon}\xi_1\sqrt{1-\alpha^2}\sqrt{1-\frac{\xi_2^2}{\xi_1^2}\alpha^2}} + \text{const} \tag{19}$$

We can recognize the standard form and we can therefore integrate and take the inverse:

$$\alpha = \text{sn}\left[\sqrt{\epsilon}\xi_1(\tau - \tau_{0,\xi}), k_\xi\right] \tag{20}$$

where the modulus k_ξ is defined by

$$k_\xi^2 = \frac{\xi_2^2}{\xi_1^2} \tag{21}$$

and $\tau_{0,\xi}$ is a constant of integration found using the initial value of ξ (F is below an elliptic integral of the first kind).

$$\tau_{0,\xi} = -\frac{1}{\sqrt{\epsilon}\xi_1} F\left[\frac{\xi_0}{\xi_2}, k_\xi\right] \tag{22}$$

Finally we can retrieve the expression of ξ (noting that α is a dummy integration variable):

$$\xi = \xi_2 \text{sn}\left[\sqrt{\epsilon}\xi_1(\tau - \tau_{0,\xi}), k_\xi\right] \tag{23}$$

In addition, the sign of the initial velocity must be taken into account (recall that we assumed positive sign in Eq. 11a and Eq. 11b). So the expression must be slightly modified by writing

$$\xi = \xi_2 \text{sn}\left[\sqrt{\epsilon}\xi_1(\delta_\xi\tau - \tau_{0,\xi}), k_\xi\right] \tag{24}$$

where

$$\delta_\xi = \text{sign}(\dot{\xi}_0 \text{cn}\left[-\sqrt{\epsilon}\xi_1\tau_{0,\xi}, k_\xi\right]) \tag{25}$$

Eq. 25 is obtained by differentiating Eq. 24 with respect to τ at initial time (noting that $\dot{\xi}_0$ and $\xi_0^{'}$ must have the same signs from Eq. 4). Another Jacobi elliptic function $\text{cn}[x,k]$ must be introduced, defined by $\text{sn}[x,k]^2 + \text{cn}[x,k]^2 = 1$. Like trigonometric functions, $\text{cn}[x,k]$ is further characterized by: $\frac{\partial \text{sn}[x,k]}{\partial x} = \text{cn}[x,k]$. The same strategy is employed for the next cases.

Regrouping all the equations of interest, the first subcase for the expression of ξ is finally:

Solution $\xi 1$:

$$\xi = \xi_2 \text{sn}\left[\sqrt{\epsilon}\xi_1(\delta_\xi\tau - \tau_{0,\xi}), k_\xi\right] \tag{26}$$

$$\text{where} \begin{cases} k_\xi^2 = \frac{\xi_2^2}{\xi_1^2} \\ \tau_{0,\xi} = -\frac{1}{\sqrt{\epsilon}\xi_1} F\left[\frac{\xi_0}{\xi_2}, k_\xi\right] \\ \delta_\xi = \text{sign}(\dot{\xi}_0 \text{cn}\left[-\sqrt{\epsilon}\xi_1\tau_{0,\xi}, k_\xi\right]) \end{cases} \tag{27}$$

Case A.1.2: $\xi_0^2 > \xi_1^2$

P_ξ takes the form:

$$P_\xi(\xi) = \epsilon(\xi_1^2 - \xi^2)(\xi^2 - \xi_2^2) \tag{28}$$

The desired canonical form of the integral is then obtained through the transformation $\xi = \frac{\xi_1}{\alpha}$. After little manipulations, the integral is reduced to:

$$\tau = \int -\frac{d\alpha}{\sqrt{\epsilon}\xi_1\sqrt{1-\alpha^2}\sqrt{1-\frac{\xi_2^2}{\xi_1^2}\alpha^2}} + \text{const} \tag{29}$$

After integration and substituting ξ into the resulting expression, we obtain:

Solution $\xi 2$:

$$\xi = \frac{\xi_1}{\text{sn}\left[-\sqrt{\epsilon}\xi_1(\delta_\xi\tau - \tau_{0,\xi}), k_\xi\right]} \tag{30}$$

$$\text{where} \begin{cases} k_\xi^2 = \frac{\xi_2^2}{\xi_1^2} \\ \tau_{0,\xi} = \frac{1}{\sqrt{\epsilon}\xi_1} F\left[\frac{\xi_1}{\xi_0}, k_\xi\right] \\ \delta_\xi = \text{sign}(\dot{\xi}_0 \text{cn}\left[\sqrt{\epsilon}\xi_1\tau_{0,\xi}, k_\xi\right]) \end{cases} \tag{31}$$

Case A.2: $\psi_\xi^+ > 0$, $\psi_\xi^- < 0$

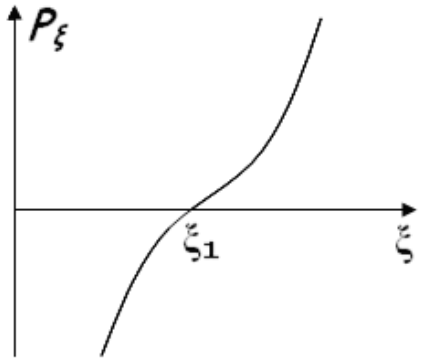

Figure 2: Representative plot of polynomial P_ξ with one real positive root.

P_ξ has two real roots and two complex conjugate roots: Let

$$\begin{cases} \xi_1^2 = \psi_\xi^+ \\ \xi_2^2 = -\psi_\xi^- \end{cases} \tag{32}$$

Using the same principle as above, from the illustrative plot of P_ξ in figure 2, the initial condition ξ_0 must satisfy the inequality $\xi_0^2 > \xi_1^2$. P_ξ takes the form:

$$P_\xi(\xi) = \epsilon(\xi^2 - \xi_1^2)(\xi^2 + \xi_2^2) \tag{33}$$

This form is again directly treated by Bowman.[44] Setting $\xi = \frac{\xi_1}{\sqrt{1-\alpha^2}}$, the integral takes the canonical form:

$$\tau = \int \frac{d\alpha}{\sqrt{\epsilon}\sqrt{\xi_1^2 + \xi_2^2}\sqrt{1-\alpha^2}\sqrt{1-\frac{\xi_2^2}{\xi_1^2+\xi_2^2}\alpha^2}} + \text{const} \tag{34}$$

Integrating and exploiting fundamental identities of elliptic functions, the expression of ξ is :

$$\boxed{\begin{array}{c}\text{Solution } \xi 3 : \\ \xi = \dfrac{\xi_1}{\mathrm{cn}\left[\sqrt{\epsilon}\sqrt{\xi_1^2+\xi_2^2}(\delta_\xi \tau - \tau_{0,\xi}), k_\xi\right]}\end{array}} \tag{35}$$

$$\text{where } \begin{cases} k_\xi^2 = \frac{\xi_2^2}{\xi_1^2+\xi_2^2} \\ \tau_{0,\xi} = -\frac{1}{\sqrt{\epsilon}\sqrt{\xi_1^2+\xi_2^2}} F\left[\sqrt{1-(\frac{\xi_1}{\xi_0})^2}, k_\xi\right] \\ \delta_\xi = \mathrm{sign}(\dot{\xi}_0 \mathrm{sn}\left[-\sqrt{\epsilon}\sqrt{\xi_1^2+\xi_2^2}\tau_{0,\xi}, k_\xi\right]) \end{cases} \tag{36}$$

Case A.3: $\psi_\xi^+ < 0$, $\psi_\xi^- < 0$

Here both zeros are complex, and the polynomial is nonnegative for all real ξ, so the solution will be valid over the entire ξ-range. Let

$$\begin{cases} \xi_1^2 = -\psi_\xi^+ \\ \xi_2^2 = -\psi_\xi^- \end{cases} \tag{37}$$

P_ξ takes the form:

$$P_\xi(\xi) = \epsilon(\xi^2+\xi_1^2)(\xi^2+\xi_2^2) \tag{38}$$

We can already note that P_ξ is always positive, so contrary to the previous cases there are no bound restrictions for the ξ-motion. Setting $\xi = \xi_2\sqrt{1-\alpha^2}/\alpha$, we may now write:

$$\tau = \int -\frac{d\alpha}{\sqrt{\epsilon}\xi_2\sqrt{1-\alpha^2}\sqrt{1-\frac{\xi_2^2-\xi_1^2}{\xi_2^2}\alpha^2}} + \text{const} \tag{39}$$

which is the desired form. After little manipulations, the expression of ξ is :

$$\boxed{\begin{array}{c}\text{Solution } \xi 4 : \\ \xi = \xi_2 \dfrac{\mathrm{cn}\left[-\sqrt{\epsilon}\xi_2(\delta_\xi \tau - \tau_{0,\xi}), k_\xi\right]}{\mathrm{sn}\left[-\sqrt{\epsilon}\xi_2(\delta_\xi \tau - \tau_{0,\xi}), k_\xi\right]}\end{array}} \tag{40}$$

$$\text{where } \begin{cases} k_\xi^2 = \frac{\xi_2^2-\xi_1^2}{\xi_2^2} \\ \tau_{0,\xi} = \frac{1}{\sqrt{\epsilon}\xi_2} F\left[\frac{\xi_2}{\sqrt{\xi_2^2+\xi_0^2}}, k_\xi\right] \\ \delta_\xi = \mathrm{sign}(\dot{\xi}_0) \end{cases} \tag{41}$$

Case B: $\Delta_\xi < 0$

In that case, $P_\xi(\psi_\xi)$ has two conjugate imaginary roots:

$$\begin{cases} \psi_\xi^+ = \frac{1}{2}(-\frac{2H}{\epsilon} + i\sqrt{\Delta_\xi}) \\ \psi_\xi^- = \frac{1}{2}(-\frac{2H}{\epsilon} - i\sqrt{\Delta_\xi}) \end{cases} \tag{42}$$

This yields to complicated expressions for the ξ-roots, and reducing the integral takes a few more steps than

the previous cases. First, we express the quartic as a product of two quadratic factors.

$$\begin{aligned} P_\xi(\xi) &= \epsilon(\xi^2 - \psi_\xi^+)(\xi^2 - \psi_\xi^-) \\ &= \epsilon(\xi - \sqrt{\psi_\xi^+})(\xi + \sqrt{\psi_\xi^+})(\xi - \sqrt{\psi_\xi^-})(\xi + \sqrt{\psi_\xi^-}) \\ &= \epsilon(\xi^2 - 2p\xi + p^2 + q^2)(\xi^2 + 2p\xi + p^2 + q^2) \\ &= \epsilon P1_\xi(\xi) P2_\xi(\xi) \end{aligned} \tag{43}$$

$$\text{where} \begin{cases} p = \frac{1}{\sqrt{2}}\sqrt{\sqrt{(\frac{H}{\epsilon})^2 - \frac{\Delta_\xi}{4}} - \frac{H}{\epsilon}} \\ q = \frac{1}{\sqrt{2}}\sqrt{\sqrt{(\frac{H}{\epsilon})^2 - \frac{\Delta_\xi}{4}} + \frac{H}{\epsilon}} \end{cases} \tag{44}$$

from the classical expression of a complex square root.

The next step is to produce a transformation that cancels the linear terms out of the two quadratics. We proceed by following the Cayley method of reduction,[44] using the generic transformation $\xi = \frac{\lambda\alpha+\nu}{\alpha+1}$. Substituting ξ in the expressions of $P1_\xi$ and $P2_\xi$, we obtain :

$$\begin{cases} P1_\xi(\alpha) = \frac{(\lambda\alpha+\nu)^2 - 2(\lambda\alpha+\nu)(\alpha+1)p + (p^2+q^2)(\alpha+1)^2}{(\alpha+1)^2} \\ P2_\xi(\alpha) = \frac{(\lambda\alpha+\nu)^2 + 2(\lambda\alpha+\nu)(\alpha+1)p + (p^2+q^2)(\alpha+1)^2}{(\alpha+1)^2} \end{cases} \tag{45}$$

We can now choose λ and ν so that the coefficients of the first power of α in the numerators of $P1_\xi$ and $P2_\xi$ will vanish:

$$\begin{cases} \lambda\nu - (\lambda+\nu)p + p^2 + q^2 = 0 \\ \lambda\nu + (\lambda+\nu)p + p^2 + q^2 = 0 \end{cases} \Rightarrow \begin{cases} \lambda = \sqrt{p^2+q^2} \\ \nu = -\sqrt{p^2+q^2} \end{cases} \tag{46}$$

After some algebraic manipulations, the integral takes the form:

$$\tau = \int \frac{2\lambda\alpha d\alpha}{\sqrt{\epsilon}AB\sqrt{\alpha^2+C^2}\sqrt{\alpha^2+1/C^2}} + \text{const} \tag{47}$$

$$\text{where} \begin{cases} C^2 = \frac{B^2}{A^2} \\ A^2 = (\lambda - p)^2 + q^2 \\ B^2 = (\lambda + p)^2 + q^2 \end{cases} \tag{48}$$

This is the same form as the previous case, so we can integrate it in the same way. Finally we can deduce from the initial transformation the fifth subcase for the expression of ξ.

$$\alpha = C\frac{\text{cn}\left[-2\sqrt{\epsilon}\sqrt{\lambda p}(\delta_\xi\tau - \tau_{0,\xi}), k_\xi\right]}{\text{sn}\left[-2\sqrt{\epsilon}\sqrt{\lambda p}(\delta_\xi\tau - \tau_{0,\xi}), k_\xi\right]} \tag{49}$$

Solution $\xi 5$:

$$\Rightarrow \xi = \lambda\frac{C\text{cn}\left[-2\sqrt{\epsilon}\sqrt{\lambda p}(\delta_\xi\tau - \tau_{0,\xi}), k_\xi\right] - \text{sn}\left[-2\sqrt{\epsilon}\sqrt{\lambda p}(\delta_\xi\tau - \tau_{0,\xi}), k_\xi\right]}{C\text{cn}\left[-2\sqrt{\epsilon}\sqrt{\lambda p}(\delta_\xi\tau - \tau_{0,\xi}), k_\xi\right] + \text{sn}\left[-2\sqrt{\epsilon}\sqrt{\lambda p}(\delta_\xi\tau - \tau_{0,\xi}), k_\xi\right]} \tag{50}$$

$$\text{where} \begin{cases} k_\xi^2 = 1 - \frac{1}{C^4} \\ \tau_{0,\xi} = \frac{1}{2\sqrt{\epsilon}\sqrt{\lambda p}} F\left[\frac{C}{\sqrt{C^2+\alpha_0^2}}, k_\xi\right] \\ \delta_\xi = \text{sign}(\dot{\xi}_0) \end{cases} \tag{51}$$

The P_η equation

In the same way as for the P_ξ equation, we first set $\psi_\eta = \eta^2$ and we compute the discriminant of the resulting quadratic polynomial:

$$\Delta_\eta = \left(\frac{2H}{\epsilon}\right)^2 - 8\frac{c-\mu}{\epsilon} \tag{52}$$

Case A′: $\Delta_\eta > 0$

In that case P_η has two real roots in ψ_η:

$$\begin{cases} \psi_\eta^+ = \frac{1}{2}(\frac{2H}{\epsilon} + \sqrt{\Delta_\eta}) \\ \psi_\eta^- = \frac{1}{2}(\frac{2H}{\epsilon} - \sqrt{\Delta_\eta}) \end{cases} \tag{53}$$

Case A′.1: $\psi_\eta^+ > 0$, $\psi_\eta^- > 0$

In that case, P_η has 4 real roots. The two positive roots satisfy:

$$\begin{cases} \eta_1^2 = \psi_\eta^+ \\ \eta_2^2 = \psi_\eta^- \end{cases} \tag{54}$$

where $\eta_1^2 > \eta_2^2$.

As for the P_ξ equation, the motion is feasible only in the regions of a space in which the condition $P_\eta > 0$ is satisfied. Noting that the quadratic coefficient of $P_\eta(\psi_\eta)$ is negative, by analogy with figure 1, it is straightforward to conclude that the initial condition η_0 must satisfy the inequalities $\eta_2^2 < \eta_0^2 < \eta_1^2$. Then we have for P_η :

$$P_\eta(\eta) = \epsilon(\eta_1^2 - \eta^2)(\eta^2 - \eta_2^2) \tag{55}$$

Setting $\eta = \eta_1\sqrt{1 - (\eta_1^2 - \eta_2^2)/\eta_1^2\beta^2}$ leads to the canonical form:

$$\tau = \int -\frac{d\beta}{\sqrt{\epsilon}\eta_1\sqrt{1-\beta^2}\sqrt{1 - \frac{\eta_1^2-\eta_2^2}{\eta_1^2}\beta^2}} + \text{const} \tag{56}$$

Using the identity $\mathrm{dn}^2 = 1 - k^2\mathrm{sn}^2$,

Solution $\eta 1$:

$$\eta = \mathrm{dn}\left[-\sqrt{\epsilon}\eta_1(\delta_\eta\tau - \tau_{0,\eta}), k_\eta\right] \tag{57}$$

$$\text{where} \begin{cases} k_\eta^2 = \frac{\eta_1^2-\eta_2^2}{\eta_1^2} \\ \tau_{0,\eta} = \frac{1}{\sqrt{\epsilon}\eta_1} F\left[\frac{\sqrt{\eta_1^2-\eta_0^2}}{\sqrt{\eta_1^2-\eta_2^2}}, k_\eta\right] \\ \delta_\eta = \mathrm{sign}(\dot{\eta}_0 \mathrm{dn}\left[\sqrt{\epsilon}\eta_1\tau_{0,\eta}, k_\eta\right]) \end{cases} \tag{58}$$

Case A′.2: $\psi_\eta^+ > 0$, $\psi_\eta^- < 0$

P_ξ has two real roots and two complex conjugate roots: Let

$$\begin{cases} \eta_1^2 = \psi_\eta^+ \\ \eta_2^2 = -\psi_\eta^- \end{cases} \tag{59}$$

Using the same principle as above, from the illustrative plot of P_ξ in figure 2, the initial condition η_0 must satisfy the inequality $\eta_0^2 > \eta_1^2$. P_η takes the form:

$$P_\eta(\eta) = \epsilon(\eta^2 - \eta_1^2)(\eta^2 + \eta_2^2) \tag{60}$$

Setting $\eta^2 = \eta_1^2(1 - \beta^2)$, we get

$$\tau = \int -\frac{d\beta}{\sqrt{\epsilon}\sqrt{\eta_1^2 + \eta_2^2}\sqrt{1-\alpha^2}\sqrt{1 - \frac{\eta_1^2}{\eta_1^2+\eta_2^2}\alpha^2}} + \text{const} \tag{61}$$

Integrating and exploiting fundamental identities of elliptic functions, the expression of η is :

Solution $\eta 2$:

$$\eta = \mathrm{cn}\left[-\sqrt{\epsilon}\sqrt{\eta_1^2+\eta_2^2}(\delta_\eta \tau - \tau_{0,\eta}), k_\eta\right] \tag{62}$$

$$\text{where} \begin{cases} k_\eta^2 = \frac{\eta_1^2}{\eta_1^2+\eta_2^2} \\ \tau_{0,\eta} = -\frac{1}{\sqrt{\epsilon}\sqrt{\eta_1^2+\eta_2^2}} F(\sqrt{1-(\frac{\eta_0}{\eta_1})^2}, k_\eta) \\ \delta_\eta = \mathrm{sign}(-\dot{\eta}_0 \mathrm{sn}\left[\sqrt{\epsilon}\sqrt{\eta_1^2+\eta_2^2}\tau_{0,\eta}, k_\eta\right] \end{cases} \tag{63}$$

Case A$'$.3: $\psi_\eta^+ < 0$, $\psi_\eta^- < 0$

This case is not physically possible, as this would lead to a negative P_η for any η.

Case B$'$: $\Delta_\eta < 0$

For the same reason as above, this case is not physically possible.

3.1.4 Summary and classification of the orbit solutions

To summarize, we obtain five different cases for ξ and two different cases for η, which leads to ten potential combinations. The general shapes of the ξ and η solutions are illustrated in figure 3 and figure 4. Note that Beletski is missing the fourth and fifth cases of ξ in his study of the problem.[36]

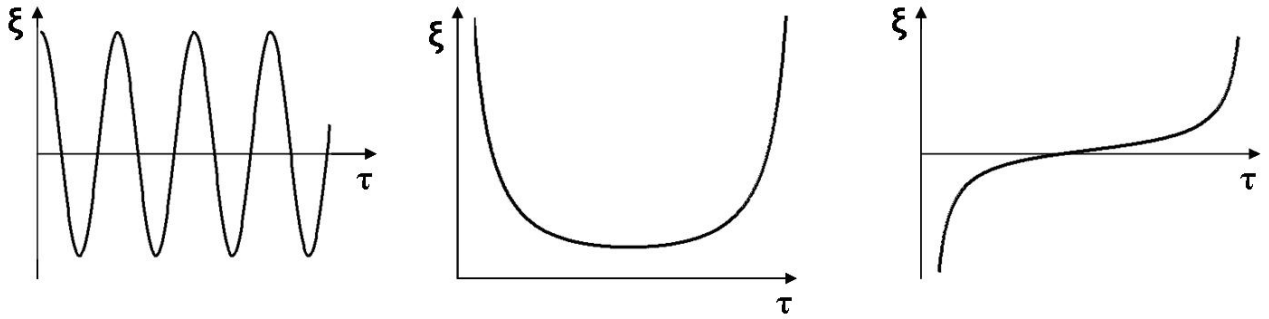

Figure 3: List of potential shapes of ξ solutions. *Left*: $\xi 1$ solution. *Center*: $\xi 2$ and $\xi 3$ solutions. *Right*: $\xi 4$ and $\xi 5$ solutions.

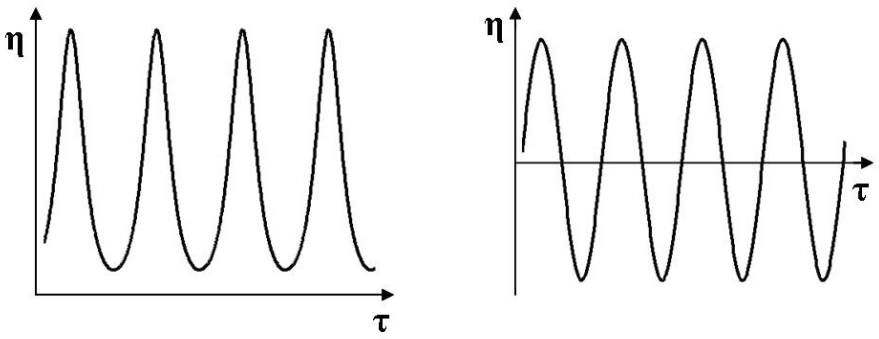

Figure 4: List of potential shapes of ν solutions. *Left*: $\nu 1$ solution. *Right*: $\nu 2$ solution.

However, not all ten combinations are feasible, their corresponding ranges of validity must overlap. To help in visualizing the distinct types of motion and their regions of validity, we construct in figure 5 a bifurcation diagram in the plane of the first integrals (H, c). The equations of the curves separating two different types

of motion are found by setting each cased variable to its relevant bound of zero and substituting into Eq. 14, Eq. 15, Eq. 52, and Eq. 53:

$$\Delta_\xi = 0 \Rightarrow \frac{c}{\mu} = -1 + \frac{1}{2}\frac{H^2}{\epsilon\mu} \tag{64a}$$

$$\Delta_\eta = 0 \Rightarrow \frac{c}{\mu} = 1 + \frac{1}{2}\frac{H^2}{\epsilon\mu} \tag{64b}$$

$$\psi_\xi^+ = 0 \Rightarrow \frac{c}{\mu} = -1 \text{ for } H > 0 \tag{64c}$$

$$\psi_\xi^- = 0 \Rightarrow \frac{c}{\mu} = -1 \text{ for } H < 0 \tag{64d}$$

$$\psi_\eta^+ = 0 \Rightarrow \frac{c}{\mu} = 1 \text{ for } H < 0 \tag{64e}$$

$$\psi_\eta^- = 0 \Rightarrow \frac{c}{\mu} = 1 \text{ for } H > 0 \tag{64f}$$

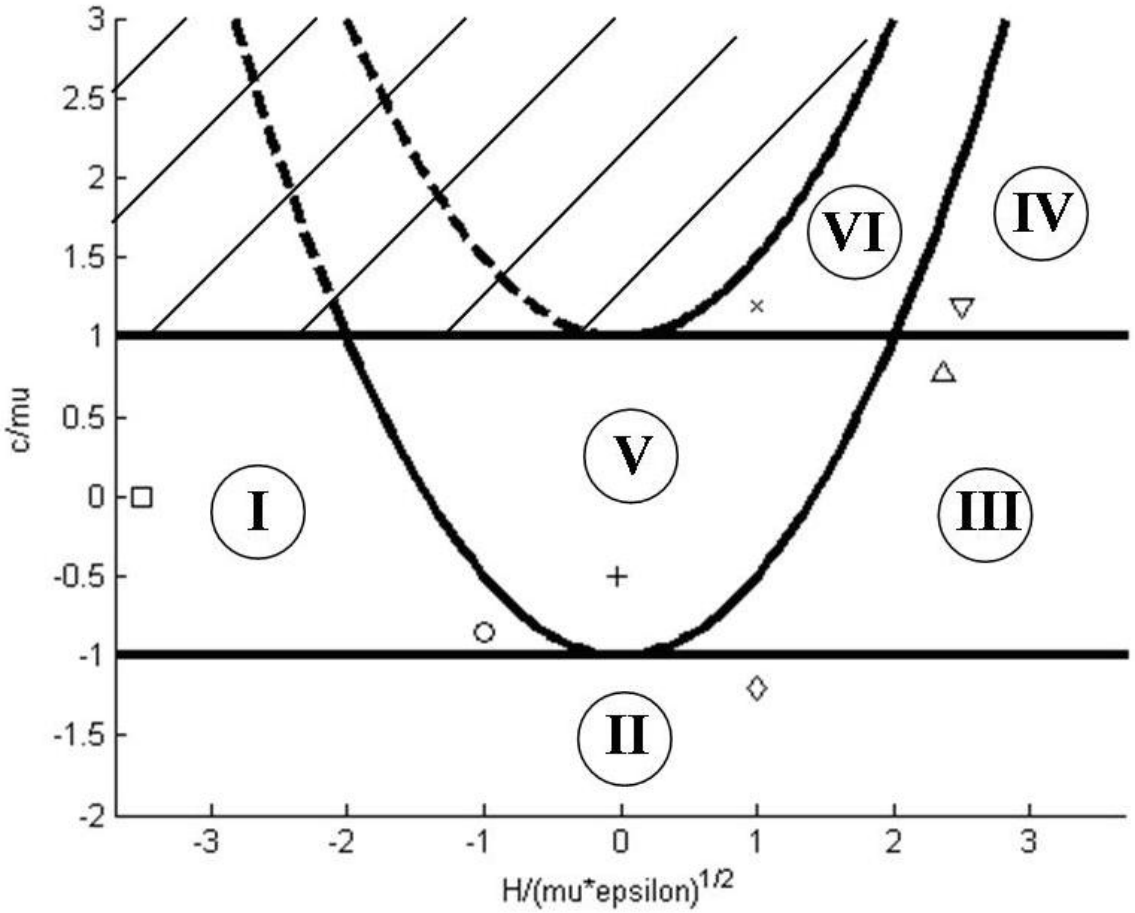

Figure 5: Bifurcation diagram of the Stark problem. Markers give the location of the illustrative trajectories of figure 6 in the diagram. *Square*: $\xi 1\eta 2$ solution. *Circle*: $\xi 2\eta 2$ solution. *Diamond*: $\xi 3\eta 2$ solution. *Up triangle*: $\xi 4\eta 2$ solution. *Down triangle*: $\xi 4\eta 1$ solution. *Plus*: $\xi 5\eta 2$ solution. *Cross*: $\xi 5\eta 1$ solution.

All in all, it turns out that six distinct domains of possible motion exist, making for seven distinct orbit types since solutions $\xi 1\eta 2$ and $\xi 2\eta 2$ are both in region I. The 2D Stark problem is therefore completely integrated. Note that the straight line $H = 0$ does not divide the bounded and unbounded motion. We may now classify all the orbit solutions that result from the appropriate combinations of ξ and η, and note the main characteristic features of the orbits in each domain of motion. Figure 6 depicts typical examples of the different orbit types.

Solutions that can be encountered for a low-thrust trajectory are mainly solutions $\xi 1\eta 2$, $\xi 2\eta 2$, $\xi 3\eta 2$, $\xi 4\eta 2$ and $\xi 4\eta 1$. In fact, a small perturbative force ($\epsilon << 1$) leads to a high absolute value for the non-dimensionalized parameter $\frac{H}{\sqrt{\epsilon\mu}}$, which corresponds to the far-left or far-right regions of the bifurcation diagram in figure 5.

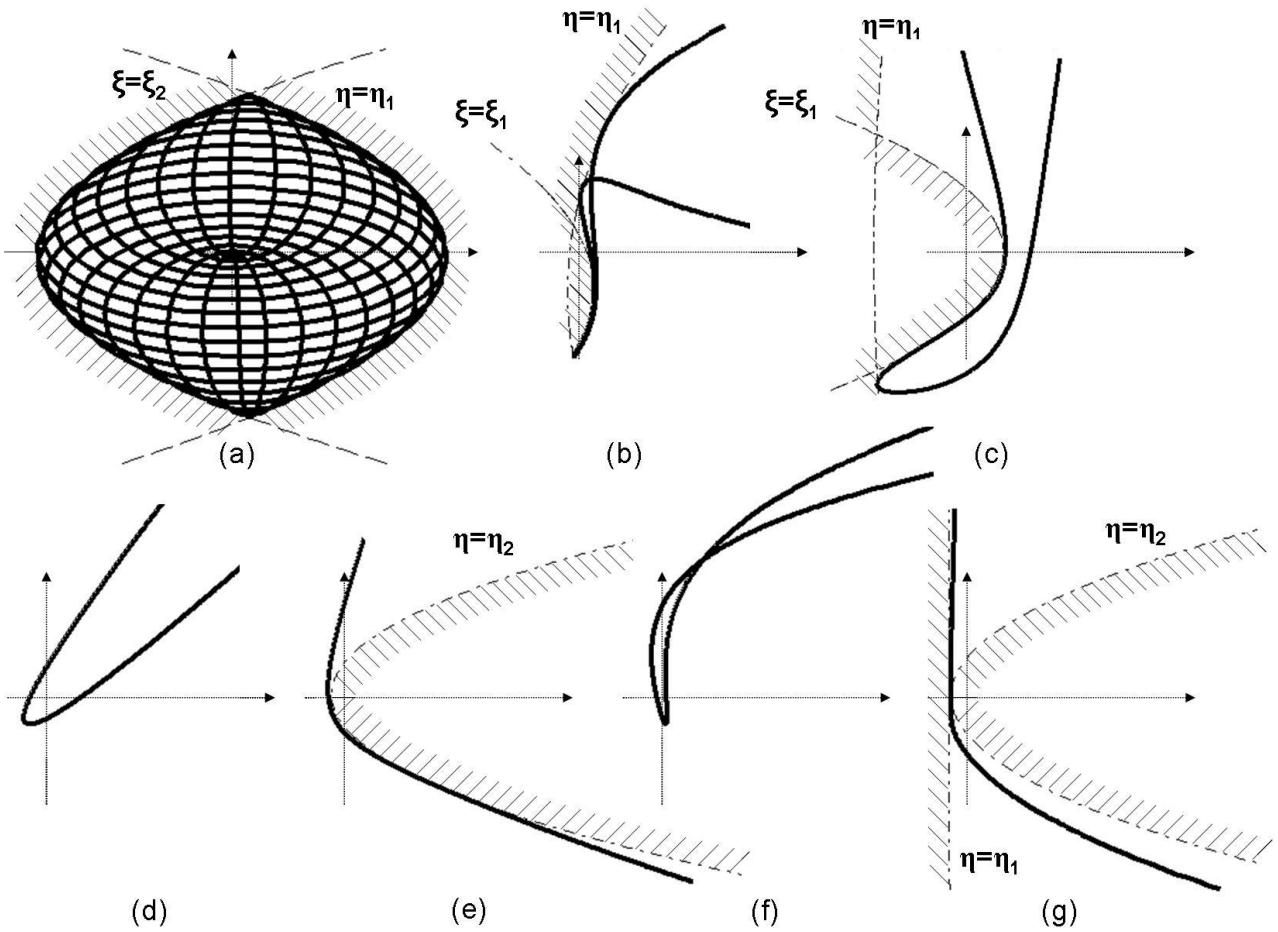

Figure 6: Typical trajectories in the x-y plane of the Stark problem. The constant force is directed along the positive x-direction. Dashed areas correspond to forbidden regions. *(a)*: $\xi 1\eta 2$ solution. *(b)*: $\xi 2\eta 2$ solution. *(c)*: $\xi 3\eta 2$ solution. *(d)*: $\xi 4\eta 2$ solution. *(e)*: $\xi 4\eta 1$ solution. *(f)*: $\xi 5\eta 2$ solution. *(g)*: $\xi 5\eta 1$ solution.

- $\xi 1\eta 2$ solution (Bounded type I)
  Motion $\xi 1\eta 2$ corresponds to a bounded orbit, and is nearly Keplerian when the constant force has a small magnitude. This lone bounded region is of most interest to the low-thrust spacecraft problem. It is restricted by the requirements $\xi < \xi_2$ and $\eta < \eta_1$. The substitution of ξ_2 and η_1 into the definitions of the cartesian coordinates yields the equations of two parabolas (plotted on figure 6) that define the boundaries of the satellite trajectory in position space.

$$x = \frac{1}{2}(\xi_2^2 - \frac{y^2}{\xi_2^2}) \tag{65a}$$

$$x = \frac{1}{2}(\frac{y^2}{\eta_1^2} - \eta_1^2) \tag{65b}$$

  It follows that the point turns around the gravitational mass, touches alternatively the two parabolas $\xi = \xi_2$ and $\eta = \eta_1$, and fills the whole space delimited by the two parabolas. Qualitatively speaking, the orbit consists of a precessing ellipse of varying eccentricity. Figure 7 illustrates the typical evolution of a trajectory shown at different times of interest. Starting with a posigrade, moderate eccentricity orbit with its line of periapsis along the direction of the constant force, the trajectory undergoes a progressive

clockwise precession and becomes increasingly radial. At the same time, the elliptical focus moves also along the y-axis until it becomes indefinitely close to the periapsis. At this point corresponding to a theoretical maximum eccentricity equal to one, the orbit switches to retrograde motion and counterclockwise precession. The orbit eventually returns to direct circulation (not shown), and the cycle continues.

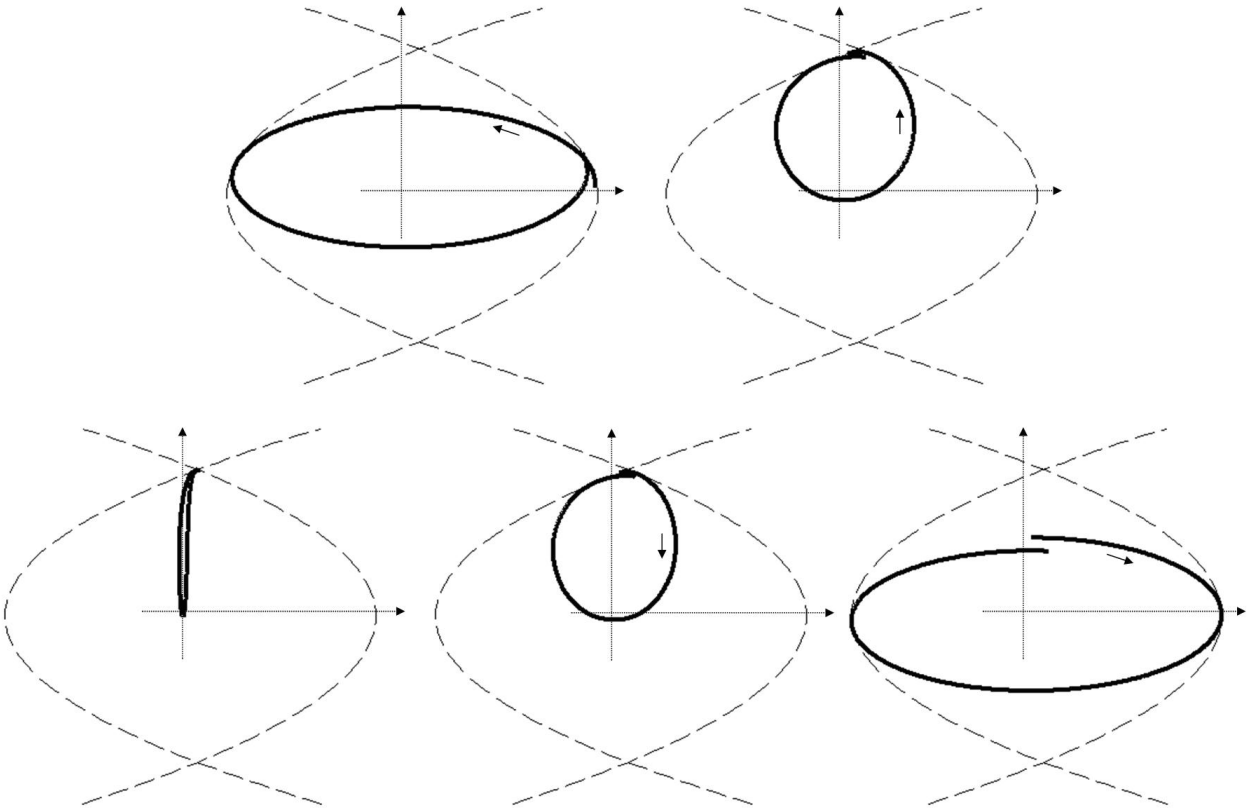

Figure 7: Typical evolution of a bounded trajectory.

- $\xi 2\eta 2$ solution (Unbounded type I)
  This type is an unbounded motion that takes place farther from the gravitational body. The zone from which orbits are excluded is defined by the equations $\xi > \xi_1$ and $\eta < \eta_1$, or in cartesian coordinates $x > \frac{1}{2}(\xi_1^2 - \frac{y^2}{\xi_1^2})$ and $x > \frac{1}{2}(\frac{y^2}{\eta_1^2} - \eta_1^2)$. As expected, the gravitational body is in the forbidden region. Close to the bounding parabola, the orbit can perform some vigorous oscillations as the point is subjected to the twin forces of attraction and exclusion.

- $\xi 3\eta 2$ solution (Unbounded type II)
  The orbit type is restricted by the same parabola as case $\xi 2\eta 2$. The point comes from infinity and returns to infinity, brushing off the parabola $\xi = \xi_1$ and $\eta = \eta_1$, without looping around the inaccessible gravitational body.

- $\xi 4\eta 2$ solution (Unbounded type III)
  This orbit is similar to the Keplerian hyperbola and has no particular characterization. The point comes from infinity, turns around the gravitational body, and returns to infinity.

- $\xi 4\eta 1$ solution (Unbounded type IV)
  The point comes from infinity, turns around the gravitational body without cutting the parabola $\eta = \eta_2$, and returns to infinity.

- $\xi 5\eta 2$ solution (Unbounded type V)
  The orbit is limited by the parabola $\eta = \eta_1$, but it is too far from the trajectory to be seen. The point comes from infinity and loops around the gravitational body in a figure-eight like pattern.